Inorganic Chemistry

ARTICLE

pubs.acs.org/IC

Aluminum Nanoparticles Capped by Polymerization of Alkyl-Substituted Epoxides: Ratio-Dependent Stability and Particle Size

Douglas W. Hammerstroem,[†] Mark A. Burgers,[†] Stephen W. Chung,[†] Elena A. Guliants,[‡] Christopher E. Bunker,[*,§] Katherine M. Wentz,[∥] Sophia E. Hayes,[∥] Steven W. Buckner,[*,†] and Paul A. Jelliss[*,†]

[†]Department of Chemistry, Saint Louis University, 3501 Laclede Avenue, Saint Louis, Missouri 63103, United States

[‡]University of Dayton Research Institute, Sensors Technology Office, Dayton, Ohio 45469, United States

[§]Air Force Research Laboratory, Propulsion Directorate, Wright-Patterson Air Force Base, Dayton, Ohio 45433, United States

[∥]Department of Chemistry, Washington University, One Brookings Drive, Saint Louis, Missouri 63130, United States

ABSTRACT: We report here on the polymerization of epoxide monomers on incipient aluminum nanoparticle cores and the effects of changing the epoxide-capping precursor and the metallic monomer ratio on the resultant stability and particle size of passivated and capped aluminum nanoparticles. When altering the ratio of aluminum to cap monomer precursor, nanoparticles capped with epoxydodecane, epoxyhexane, and epoxyisobutane show a clear decreasing trend in stability with decreasing alkane substituent length. The nanoparticle core size was unaffected by cap ratio or composition. PXRD (powder X-ray diffraction) and DSC/TGA (differential scanning calorimetry/thermal gravimetric analysis) confirm the presence of successfully passivated face-centered cubic (fcc) aluminum nanoparticles. We also report preliminary results from ATR-FTIR (attenuated total reflectance-Fourier transform infrared), ^{13}C CPMAS (cross-polarization/magic-angle spinning), and ^{27}Al MAS solid-state NMR (nuclear magnetic resonance) measurements. The most stable aluminum nanoparticle−polyether core−shell nanoparticles are found at an Al:monomer mole ratio of 10:1 with an active Al^0 content of 94%.

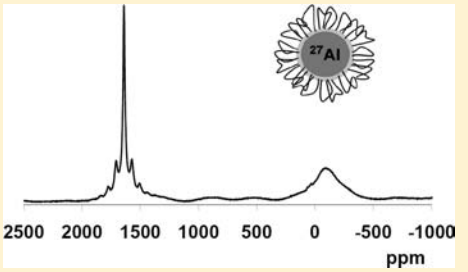

INTRODUCTION

Metallic aluminum particles readily react with air and water to form aluminum oxide (Al_2O_3), processes which involve the evolution of a large amount of hydrogen gas and heat. Both of these processes have significant technologic utility, with applications for both small-scale hydrogen production and high-density energy storage.[1]

Micrometer-sized aluminum particles are more easily produced and stored but have disadvantages with respect to aluminum nanoparticles (Al NPs). Micrometer-sized particles do not oxidize as fully or quickly; therefore, they produce less hydrogen gas and heat per gram of Al. Aluminum NPs have demonstrated faster burn rates, lower activation energy for H_2 absorption and desorption, and potential for higher energy release and will oxidize more fully and quickly, thus providing better performance relative to micrometer scale particles. However, there are significant challenges when moving to the nanoscale. Aluminum particles exposed to air undergo rapid aging to produce a 2−6 nm thick oxide shell.[2] For micrometer-scale aluminum particles, this oxide shell may account for <0.5% of the particle mass, but for Al NPs with diameters <20 nm the oxide layer can account for >70% of the particle mass. For the Al NPs this oxide layer results in a much lower energy density. In addition, thicker oxide layers result in particles with elevated temperatures for ignition.[3−5]

To address these challenges, passivation schemes that prevent or mitigate oxide shell formation are under investigation. These schemes include protection of the nascent Al NPs with graphite,[6] polymers,[7] carboxylic acids,[8,9] and transition metals.[10] These capping schemes have demonstrated both limited air stability and control over particle size distribution, typically producing non-pyrophoric particles in the average range of 50−200 nm in diameter. Previously, we reported on the synthesis of Al NPs produced by Buhro's synthetic method and followed by capping and passivation by addition of alkyl-substituted epoxides.[11,12] The epoxides undergo ring-opening polymerization to produce polyether caps that stabilize the nascent Al NPs from subsequent aggregation and oxidation in air. Here we discuss the relationship between the Al NP precursor alane-to-epoxide monomer cap ratio and the resultant stability and size of our epoxide-capped particles. We also describe the use of sonochemical treatment during synthesis and its impact on the resulting Al NPs.

EXPERIMENTAL SECTION

Reagents and Materials. *N,N*-Dimethylethylamine alane ($H_3Al\cdot NEtMe_2$, 0.5 M) solution in toluene, titanium(IV) isopropoxide

Received: February 17, 2011
Published: May 12, 2011

(99.999% trace metals basis), 1,2-epoxyisobutane (97%), 1,2-epoxyhexane (97%), 1,2-epoxydodecane (95%), ethylenediaminetetraacetic acid disodium salt dihydrate (~99%), and zinc sulfate heptahydrate (99.999%) were all supplied by Sigma-Aldrich. Toluene was distilled over sodium metal under a dry argon atmosphere in order to remove water and oxygen. Alane solutions, purchased from Sigma-Aldrich, were stored under argon to prevent oxygen exposure.

Synthesis. All wet chemical reactions were completed using a dry, air-free reaction flask under an argon atmosphere on a Schlenk line at room temperature stirring rapidly using a magnetic stirrer. A 13 mL amount of alane (0.0065 mol) and 10 mL of toluene were injected into the flask using a Luer lock syringe. A stoichiometric amount of epoxide was added as the capping agent. For each capping agent, 1:1, 2:1, 4:1, 6:1, 8:1, 10:1, and 12:1 molar ratios of alane:epoxide were investigated. Finally, 10 μL of titanium isopropoxide catalyst was added to the alane mixture, turning the clear colorless mixture to a dark-brown to black mixture. The reaction was allowed to stir for approximately 1 min. After 1 min, the excess solvent was removed in vacuo while stirring at room temperature. The resultant product was then left in vacuo overnight.

For the sonochemical synthesis a 10:1 Al:epoxydodecane molar ratio was used. For each synthesis, 10 mL of a 0.5 M alane solution was used. Epoxydodecane was dissolved in decane to produce 4 mL of solution that was subjected to five cycles of a freeze−pump−thaw process to remove dissolved oxygen. The alane and epoxydodecane solutions were mixed to produce 14 mL of total solution with an Al:epoxide of 10:1. Titanium(IV) isopropoxide catalyst (16 μL) was added to this solution and transferred to a sonication flask (Sonics Inc., Suslick flask). Sonication was performed in a nitrogen-filled glovebag encompassing the sonication instrument (Sonics Inc., Vibra Cell). The instrument consisted of a 0.5 in. diameter solid titanium horn operated at 20 kHz. The solution was sonicated for 7.5 min active time at an amplitude of ~22 W using a 1-s-on, 1-s-off procedure. The bulk reaction solution reached a maximum temperature of 70 °C. The resultant black solution gradually precipitated, yielding a grayish-black powder, which was recovered by evaporation of the solvent under vacuum followed by repeated washings with hexane and drying under an N_2 stream.

PXRD. PXRD (powder X-ray diffraction) analysis was performed on a Bruker D8-Advanced equipped with a Cu Kα source, monochromator, and Sol-X detector. The presence of fcc Al or crystalline Al_2O_3 was determined by comparison to the ICDD Crystallographic Database.

DSC/TGA. The presence of passivated face-centered cubic (fcc) Al NPs was confirmed using a TA Instruments STD Q600 dual DSC/TGA (differential scanning calorimetry/thermal gravimetric analysis) instrument with open pan alumina sample cups. Samples were analyzed from room temperature to 800 °C using a 10 °C/min temperature profile under a constant flow of air.

NMR. Solid-state NMR measurements were conducted in a 4 mm Varian solids NMR probe using rotors equipped with special caps for handling air-sensitive samples such as these. $^{13}C\{^1H\}$ CPMAS experiments were performed at MAS rotational frequencies of 5 kHz, with a ^{13}C observe frequency of 74.02 MHz, and ^1H decoupling frequency of 294.38 MHz. Typical $\pi/2$ pulses were 3 μs and a contact time of 2 ms with recycle delays of 3s. ^{27}Al experiments were recorded with MAS rotational frequencies of 5 kHz at an observe frequency of 76.72 MHz. In order to simultaneously record Al^0 and Al^{3+} regions of the spectrum, a Bloch decay sequence (pulse length of 2 μs) was used with the carrier frequency centered midway between these two regions. Recycle delays were 1 s.

Active and Total Aluminum Content Determination. Determination of the active aluminum content was carried out using a previously described method.[13] The Al NPs (0.045 g) synthesized from the 10:1 epoxydodecane−alane batch were treated with an excess of 5 M NaOH(aq) solution in a retort, which was connected to a sealed manometer. The released H_2 was evolved into a manometer filled with a saturated NaCl aqueous solution to minimize the H_2 dissolution. The released H_2 volume was quantified and used to calculate active Al. Moles of active aluminum = 5.844×10^{-4} mol corresponding to 0.016 g of Al^0 (35%).

Total Al content was determined using a complexometric back-titration method.[14] Concentrated HNO_3(aq) was added to the aluminum NaOH mixture remaining after H_2 evolution. The mixture was diluted into a 500 mL volumetric flask, and then 10 mL of a 0.05 M secondary standard solution of EDTA (ethylenediaminetetraacetic acid disodium salt dihydrate) was added to 50 mL of the aluminum solution. The solution was then brought to a pH of 7 followed by addition of 10 mL of a pH 5 acetate buffer. The solution was heated to a boil for 5 min to ensure complete complexation of all Al and was then back-titrated using a primary standard zinc sulfate heptahydrate solution with xylenol orange indicator (yellow → pink). Moles of total aluminum = 6.222×10^{-4} mol.

RESULTS AND DISCUSSION

Alane decomposes in the presence of catalytic amounts of titanium isopropoxide according to eq 1.[11]

$$2AlH_3(\text{toluene}) \rightarrow 2Al(s) + 3H_2(g) \quad (1)$$

Decomposition and its associated color change is instantaneous with the solution turning from clear to dark-brown. In the absence of a cap that inhibits agglomeration, decomposition of alane continues uncontrolled until a metallic bulk aluminum mirror deposits on the surface of the inside of the reaction flask. After removal of solvent in vacuo, the material is a mixture of pyrophoric cubic and polygonal particles that are 350−500 nm in diameter.

However, following addition of an epoxide cap (epoxyisobutane, epoxyhexane, or epoxydodecane), the material is no longer pyrophoric and demonstrates varying degrees of stability dependent upon the epoxide cap used and its ratio. As previously described, alane decomposition yields metallic aluminum particles.[12] The incipient Al NPs serve as a site for initiation of polymerization of the epoxide monomer. This is not unreasonable given the known ring-opening reduction of epoxides by alkali metals to produce alkoxide−carbanions.[15] The transient surface alkoxide−carbanion would be expected to preferentially bind to the partially oxidized metal surface via the oxygen rather than the carbon, leading to carbanionic attack on the next epoxide monomer in the solvent to set off the polymerization cascade. This will create a putative butane−dioxy loop, whereupon propagation would then be expected to lead to outgrowth of a monolayer of polyether loops from the Al NP core surface, based on a concerted mechanism in which the epoxide monomer is inserted into an Al−O bond (Figure 1).[16,17] This would in theory create a polymer cap with no exposed end groups and a polyether cap outer surface as well as polyether cap interior. Thus, termination effectively occurs by virtue of limited monomer supply to the Al NP surface, which may be more a function of diminished diffusional mobility, rather than an exhaustion of the bulk solution content.

The resultant alkyl substituents on the polyether chain vary in length dependent on the cap used. This general procedure was repeated with all caps with varying reaction times ranging from less than a minute to 72 h. We also investigated the effect of addition of cap to the reaction mixture after Al NP formation, versus Al NP formation in the presence of the capping agent in solution. In both cases, PXRD and DSC/TGA showed no discernible difference in particle size or stability. As a result, all

dx.doi.org/10.1021/ic2003386 |Inorg. Chem. 2011, 50, 5054–5059

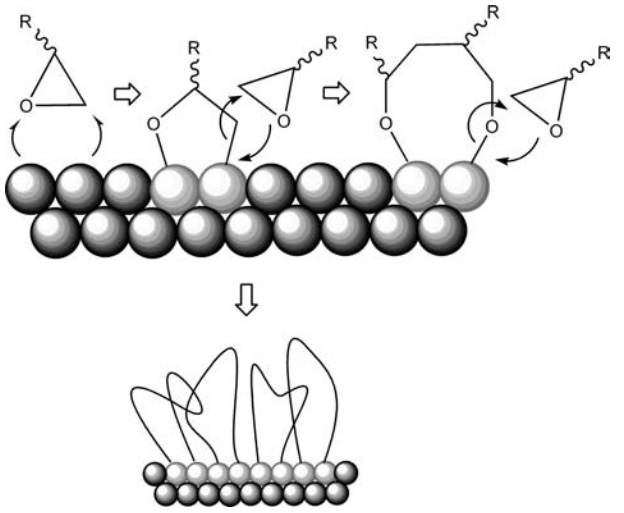

Figure 1. Conceptual view of initiation and propagation of polymer chain growth at the Al core−cap interface. Light gray spheres represent surface-oxidized Al.

reactions discussed here were performed with a cap already in solution. After reaction (∼5 s) the reaction mixture was placed under vacuum to remove the solvent while stirring. This process required ∼1 h. Samples were left under vacuum overnight, at which point they were placed under inert atmosphere until analysis.

Each cap at each ratio yielded a dark-gray to black product with a waxy consistency being more prevalent in epoxyisobutane and more tarlike in epoxydodecane. For 1:1 and 12:1 ratios, all caps produced unstable particles upon exposure to air, with extremely rapid oxidation or ignition. Visual observation of Al_2O_3 powder formation upon air oxidation was confirmed by PXRD. With epoxyisobutane, the product was entirely unstable at all ratios with varying degrees of pyrophoricity, ranging from rapid oxidation to ignition when exposed to air. With epoxyhexane, all ratios in the 2:1 to the 10:1 range were not pyrophoric but all rapidly oxidized in the order of minutes, with the 10:1 ratio oxidizing the slowest. Poly(epoxydodecane)-capped materials demonstrated the greatest air stability overall. Thus, there is a clear trend in increasing Al NP core stability with increasing hydrocarbon substituent length. This observation is consistent with recent results that suggest that Al NPs are much more reactive toward water than toward oxygen.[18] The large hydrophobic side chains on the polyether cap structure protect the core from water more effectively. It is possible that the polyether chains themselves can act as a conduit for water diffusion to the core, so the hydrocarbon side chains play a critical role in creating a more hydrophobic environment around the reactive Al NP core.

We investigated the stability and particle size effects using the epoxydodecane monomer in more detail. PXRD was used to determine the presence of fcc aluminum. When capping and passivation of the Al NP core was successful, fcc Al peaks are observed. However, if capping and passivation were not successful, oxidized aluminum existing in an amorphous mixture of boehmite, bayerite, and corundum was produced. At a 2:1 ratio, epoxydodecane yielded a nonpyrophoric material, which fully oxidized within 10 min of air exposure. For the 4:1 to the 10:1 ratios, PXRD revealed the presence of fcc Al peaks with increasing relative intensity for the higher alane:cap ratios as shown in

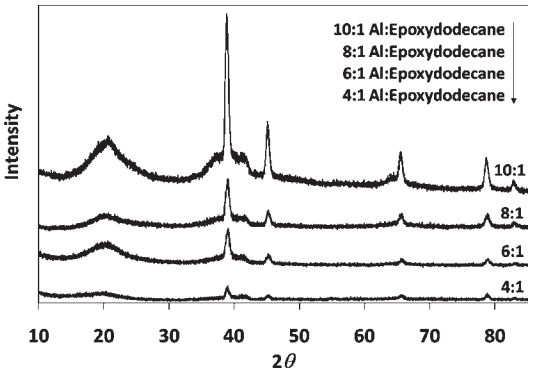

Figure 2. PXRD patterns of polymer-capped Al NPs at varying Al:epoxydodecane ratios. All PXRD patterns are shown on the same scale of intensity. Peaks at 2θ = 38.8°, 45.1°, 65.4°, 78.6°, and 82.8° are attributed to fcc Al.

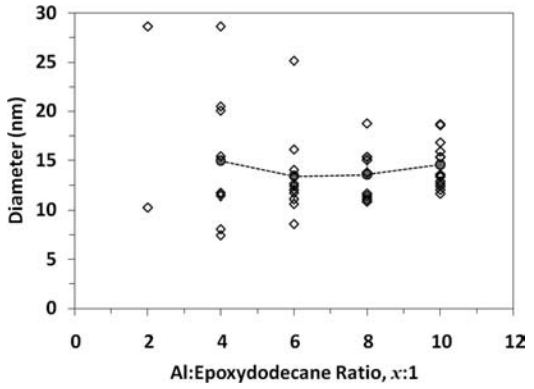

Figure 3. Epoxydodecane-capped particle sizes at 2:1, 4:1, 6:1, 8:1, and 10:1 Al:epoxydodecane molar ratios. Data points were calculated using the Scherrer equation on half-height peak-width measurements from up to three separately measured PXRD patterns. The gray-circled data points linked by a dotted line represent the mean size for calculated diameter values from each set of PXRD peaks. With only two measurable data points, a mean value for the 2:1 ratio was not determined.

Figure 2. Broad peaks observed at about 2θ = 20° are believed to emanate from the amorphous polyether cap.

The sizes of the Al NP cores were determined using PXRD and the Scherrer equation. Figure 3 shows results for the full range of Al:cap ratios for a series of replicates at each cap ratio. We find that as the alane:cap ratio increases, the distribution in particle size narrows, with our most stable ratio (10:1) yielding the narrowest distribution. At lower Al:cap ratios, where the capping agent concentration is higher, the median Al NP size remains the same but there are samples with significantly larger and smaller diameters. This large variation may be due to the increase in solution viscosity at high cap concentrations. Higher viscosities may lead to less effective reagent mixing and thus greater embryo and nuclei nonuniformity both in size and in local reaction environment. This would produce a wider range of Al NP core sizes before initiation of polymerization capping. Once capping initiates, the Al NP core growth ceases. However, the mean size for each range of samples is not discernibly affected by the Al:cap ratio. Thus, for ratios 4:1, 6:1, 8:1, and 10:1, the mean PXRD-peak diameter values were determined to be 15, 13, 14, and 15 nm, respectively. This is in contrast with our previous

dx.doi.org/10.1021/ic2003386 |*Inorg. Chem.* 2011, 50, 5054–5059

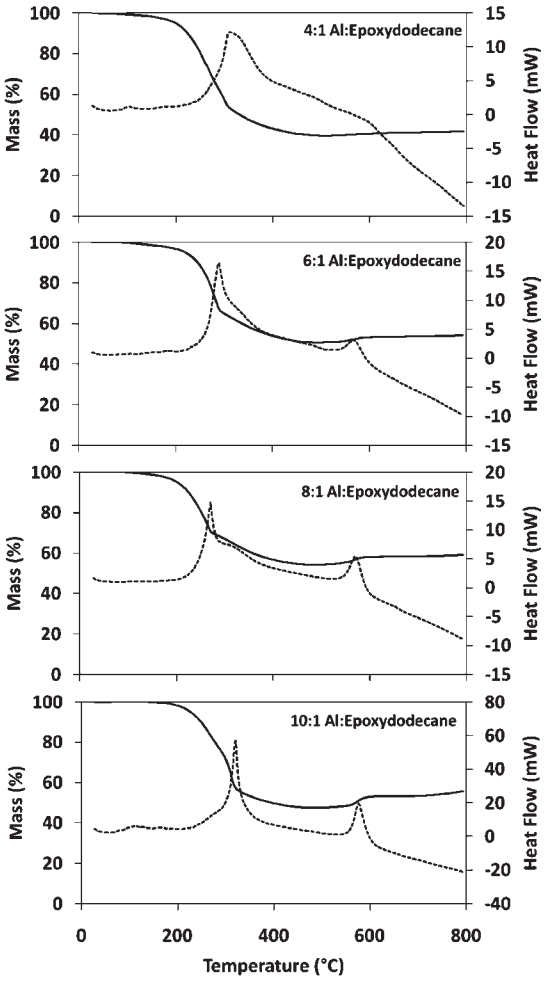

Figure 4. DSC (dotted line) and TGA (solid line) of epoxydodecane-capped Al NPs at varying ratios.

observations where time of addition of cap dramatically changes the mean Al NP core size.[12]

Our previous TEM observations and size measurements produced an average particle diameter of 20−30 nm, but these clearly included the capping layer with the Al core.[12] Since PXRD peak widths should only be a function of crystallite size, the polymer shell should not contribute. This suggests an approximate polymer capping thickness of ∼5−15 nm. This formally represents a lower limit, although we anticipate that our Al NPs are not at all polycrystalline given the time scales of NP formation, growth, and capping. The latter phenomenon is expected to happen long before the Al NPs have grown sufficiently large enough to create grain boundaries.

DSC/TGA was also used to confirm the presence of active aluminum with results shown in Figure 4. Polyether cap ignition is expected around 300 °C in the DSC with an associated mass loss in the TGA. At this point, it is assumed the organic cap is combusted and Al NPs with a monolayer oxide shell remain. TGA shows that all samples lose between 50% and 60% of their mass up to 450 °C by the time the cap is burnt off, suggesting that a little over one-half the mass of the Al NPs can be attributed to the polyether cap. Aluminum ignition is expected at ∼560 °C with an associated mass increase on oxidation due to formation of the heavier oxide.[19] For 4:1 and 6:1 ratio samples, there was very

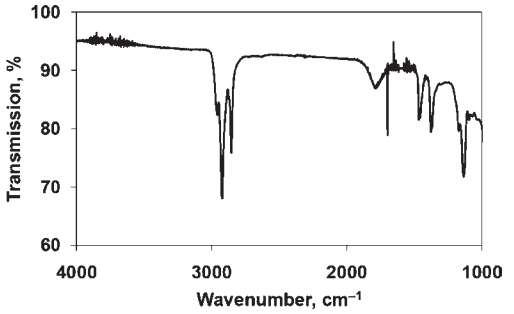

Figure 5. ATR-FTIR spectrum of 10:1 Al:epoxydodecane Al NPs.

little associated mass gain at these higher temperatures. This may indicate that for these systems the Al NP ignition occurs over a range of lower temperatures. Indeed, DSC peaks corresponding to polymer combustion are coincident with inflection points in the TGA trace, leading to a discernible deceleration in mass loss prior to leveling off. This may well be attributed to Al combustion (to Al_2O_3) partially offsetting mass loss due to the polyether cap combustion. For the 8:1 and 10:1 ratio samples, there is a significant mass gain observed at higher temperatures and a sharp ignition peak in the DSC traces for reaction of the Al NPs. For the 8:1 ratio sample, the DSC shoulder at 280 °C (and corresponding adjustment in TGA trace slope) is still quite well defined. For the 10:1 ratio sample, however, we conclude the polyether cap and Al combustions are distinct, temperature-separated events (320 and 570 °C), albeit with a DSC peak at a somewhat higher temperature than for the other three samples. Despite these well-defined ignition characteristics, we note for the 10:1 sample a gradient inflection in the TGA prior to cap ignition at ∼270 °C associated with a shoulder in the DSC trace to the low-temperature side of the cap ignition peak. This is most likely due to the presence of some unpolymerized epoxide monomer and its subsequent desorption and combustion, a result confirmed by solid state ATR-FTIR and NMR spectroscopic studies (vide infra).

ATR-FTIR Spectroscopy. The ATR-FTIR spectrum of a solid sample of 10:1 epoxydodecane-capped Al NPs is shown in Figure 5. Previous assignment of C−H bands in poly(propylene oxide) suggests the strongest resonances at 2920 and 2850 cm^{-1} are $\nu_{antisym}(CH_2)$ and $\nu_{sym}(CH_2)$ stretching modes, with the weaker peaks at 2960 and 2865 cm^{-1} associated with the corresponding CH_3 stretches.[20] A resonance at 1370 cm^{-1} may likewise be attributed to overlapping CH_2 and CH_3 deformations. Of most interest are strong- and medium-intensity bands observed at 1130 and 1460 cm^{-1}, respectively. The lower one emanates from polyether CH_2-O-CH_2 stretching vibrations, and we believe the absorption at 1460 cm^{-1} is due to the presence of unreacted epoxide trapped in the outer polyether matrix. This is supported by solid state CPMAS ^{13}C NMR spectroscopy (vide infra).

Solid-State MAS and CPMAS NMR Spectroscopy. Once dried, the 10:1 Al:epoxydodecane NPs neither are appreciably soluble in any solvent nor do they disperse easily in any fluid medium. This makes procurement of routine solution NMR spectra problematic. Solid-state NMR spectroscopy, however, could be used to probe structural details of the cap and the oxidation state of the Al core, as well as the core−cap interface.

The ^{27}Al MAS NMR spectrum for a 10:1 Al:epoxydodecane Al NP sample is shown in Figure 6, which confirms that the epoxide

dx.doi.org/10.1021/ic2003386 |Inorg. Chem. 2011, 50, 5054–5059

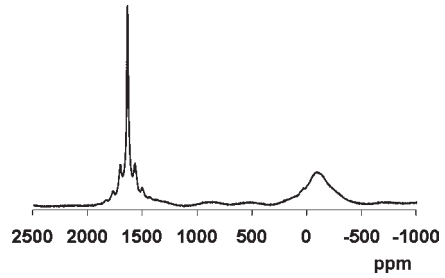

Figure 6. ^{27}Al MAS NMR spectrum of 10:1 Al:epoxydodecane Al NPs (at 300 MHz, 5 kHz spinning).

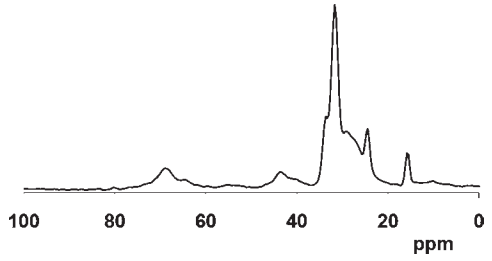

Figure 7. ^{13}C CPMAS NMR spectrum of 10:1 Al:epoxydodecane Al NPs (300 MHz magnet, 5 kHz spinning).

cap provides a protective layer that (temporarily) prevents complete oxidation of the metallic Al NP's. ^{27}Al is a quadrupolar nucleus ($I = 3/2$) and is subject to broadening interactions due to electric field gradients at noncubic Al sites. The prominent Knight-shifted feature at δ 1641 ppm is indicative of an Al^0 metallic species which is shown in coexistence with one or more Al^{3+} species indicated by broad overlapping features centered at −70 ppm. The Al^0 resonance is flanked by rotational resonances from magic-angle spinning conditions. Notably, the metallic Al feature will disappear after the sample has been in air for several days (data not shown.) With these preliminary data, it cannot be confirmed whether the broad feature at low frequency is due to one or more overlapping resonance. Such resonances could be attributable to species at the core−cap interface such as Al−oxide or Al−hydride material trapped from the alane reagent; both could be expected to resonate in this vicinity. Complicating factors in these measurements have been a small Al background arising from the zirconia rotor that resonates in the vicinity of 0 ppm and the air-sensitive nature of the samples (limiting the duration of possible experiments that can be performed). Nevertheless, additional studies are underway to elucidate these overlapping features and to assess first-order and second-order quadrupolar broadening of the sites.

The $^{13}C\{^1H\}$ CPMAS NMR spectrum for the same 10:1 Al:epoxydodecane Al NPs is shown in Figure 7. The spectrum provides evidence for reacted epoxydodecane, with some evidence of the presence of unreacted monomer. Two broad sets of overlapping resonances are observed in the solid-state NMR spectrum at δ 63−68 ppm and 39−43 ppm. Both of these broad resonances are attributable to oligomerization or polymerization of the epoxide; they are absent from comparable solution-phase spectra of the unreacted epoxide monomer. The higher frequency group is consistent with sp^3 carbons associated with ethers such as those found in polyprolyene oxide, $-CHR-CH_2-O-$. The group of resonances at 39−43 ppm is consistent with CH_2 species similar to polypropylene such as may be found in the purported butanedioxy loop. At this time, we cannot assign this feature with certainty. The broadness of the peaks and lack of resolution between CH_2 and CHR carbons likely reflects the absence of stereo- and regiocontrol in the chain, leading to random conjoining of monomers in a head-to-head, head-to-tail, or tail-to-tail arrangement. The solid-state CPMAS spectrum also appears to have features in common with those of the liquid-phase epoxydodecane monomer, with very sharp resonances observed for ^{13}C in the solid state, attributable to the long alkyl 10-carbon side chain, resonating between ∼33 and 14.6 ppm, but notably, a very weak feature is observed in the baseline of the ^{13}C spectrum that would be consistent with the epoxide ring at 52.3 ppm (for CHR). The small size of the signal could be due to experimental difficulties with cross-polarization dynamics; more work is needed to fully investigate this aspect of the spectrum.

No shifted resonances from association between the ^{13}C and the metal surface are observed within the spectral window from δ 712 to −639 ppm, confirming that there are no resolvable metal−carbon bonds in the Al NPs. Tsang reported, albeit for solution ^{13}C NMR spectroscopic analysis of PVP-stabilized Ru nanoparticles (PVP = poly(vinylpyrrolidone)), that for metal nanoparticle-bound organic molecules the Knight shift is completely eliminated when metal and carbon atoms are separated by as little as one oxygen atom (as in the bound formate species studied) and the one proposed here.[21]

Total and Active Al Content. The Al NPs were analyzed for both total aluminum content and active (as zerovalent Al^0) content. A hydrogen emission study, where all active Al^0 was decomposed in aqueous solution (based on $2Al^0$:$3H_2$ stoichiometry), determined that the Al NPs contained ∼35% Al^0 by mass, in reasonable agreement with the TGA results discussed above. This compares very favorably with the value of ∼15% determined for perfluorotetradecanoate-capped Al NPs capped reported by Jouet et al. and ∼40% for oleate-capped Al NPs prepared by Bunker et al.[8,22] Through total aluminum analysis, the active Al content (Al^0 relative to total Al in any oxidation state) was determined to be 94%, which is extremely high for Al NPs of these dimensions.

Sonochemical Synthesis. Sonochemistry has been previously used for the synthesis of passivated Al NPs, with the resulting nanoparticles demonstrating long-term air stability.[22] A variety of organic molecules were investigated using the sonochemical method, with oleic acid being the most successful capping agent. Following the methods of Bunker et al.,[22] epoxydodecane was used in a 10:1 ratio in place of the oleic acid capping agent. The objective was to investigate the difference between a nonsonochemical synthesis in toluene at room temperature (as described above) and a sonochemical synthesis in decane which reaches a bulk solution temperature of ∼70 °C. Both experiments returned products with very closely matched PXRD patterns, displaying similar signal-to-noise ratios (Figure 8). The peak widths of signals for the sonochemically produced Al NPs are, nevertheless, perceptibly broader than those produced without irradiation. Application of the Scherrer equation to the four strongest peaks observed in either PXRD pattern suggested that the sonochemically produced Al NPs were 11 nm in diameter (on average) versus 16 nm as determined from the PXRD pattern for nonsonochemically produced Al NPs.

The most notable difference between sonochemically and nonsonochemically produced samples was observed in DSC/TGA measurements (Figure 9). For the Al NPs produced by the sonochemical method, a lower temperature onset (<200 °C) for

dx.doi.org/10.1021/ic2003386 |Inorg. Chem. 2011, 50, 5054–5059

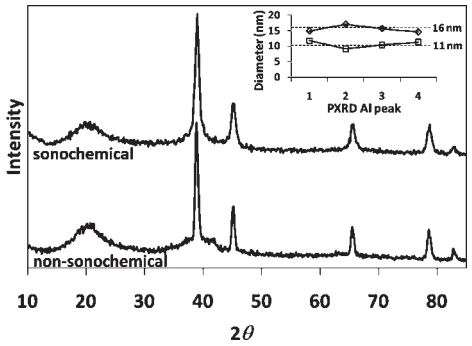

Figure 8. PXRD patterns for sonochemically produced and nonsonochemically produced Al NPs. (Inset) Particle diameters as determined by application of the Scherrer equation to the four strongest fcc Al peaks at $2\theta = 38.8°$ (peak 1), 45.1° (peak 2), 65.4° (peak 3), and 78.6° (peak 4); data for sonochemically (□) and nonsonochemically (◊) produced Al NPs.

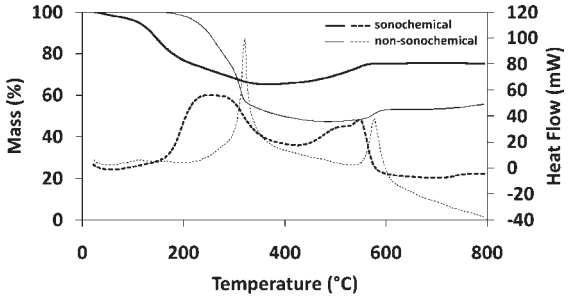

Figure 9. DSC (dotted lines) and TGA (solid lines) comparison of sonochemical (thick lines) and nonsonochemical (thin lines) synthetic techniques.

the capping agent loss and combustion is noted in both DSC and TGA. TGA shows only a 35% loss in mass (compared with 50% for the nonsonochemically produced Al NPs), and this occurs over a broader temperature range. The DSC peak is substantially broader also. This would seem to suggest that in the case of poly(epoxydodecane)-capped Al NPs, sonochemical irradiation has disrupted the cap-forming process, laying down an inhomogenous polymer layer, one which may contain smaller oligomer units or perhaps even more unreacted epoxide monomer. Whether this process is directly sensitive to the sonication or the resulting temperature increase has yet to be determined. The consequence for ensuing Al ignition (and oxide formation) is also apparent, with a broad shoulder at 510 °C and a final ignition peak at 540 °C. TGA shows mass increase due to oxide formation commencing as low as 400 °C. Premature Al ignition may be occurring if the cap−core interface is compromised in some of the NPs leading to a smaller surface layer and a lower activation barrier to ignition. This observation again suggests that sonication exerts a more disruptive effect on the NP core−cap assembly.

CONCLUSIONS

Nonpyrophoric Al NPs are produced by synthesis of an Al NP core followed by capping with a polyether produced by polymerization of an epoxide on the nascent Al NP. The stability of the Al NP core is strongly dependent upon the epoxide alkyl substituent as well as the ratio of Al:epoxide monomer. Epoxyisobutane does not produce stable core−shell nanoparticles, and epoxyhexane produces core−shell nanoparticles with stability that is limited to less than 1 h. Epoxydodecane yields the most stable core−shell nanoparticles, with significant quantities of active aluminum as evidenced by PXRD, ^{27}Al MAS NMR, and DSC/TGA. There is no discernible difference in the resulting material for immediate addition of the cap versus when the cap is already in solution. While the length of alkyl substituent on the epoxide cap seems to have no effect on particle size, an increased alane:cap ratio yields a narrower distribution in particle size. An optimal ratio of the Al:epoxydodecane appears at 10:1. The very high active Al^0 content (35% of total NP mass, 94% of total Al content) measured for this product is particularly desirable for high-energy material applications.

AUTHOR INFORMATION

Corresponding Authors

*E-mail: jellissp@slu.edu, buckners@slu.edu.

ACKNOWLEDGMENT

We gratefully acknowledge the Air Force Research Laboratory Nanoenergetics Program for supporting this work.

REFERENCES

(1) Ramaswamy, A. L.; Kaste, P. *J. Energy Mater.* **2005**, *23*, 1.
(2) Aumann, C. E.; Skrofronick, G. L.; Martin, J. A. *J. Vac. Sci. Technol. B* **1995**, *13*, 1178.
(3) Trunov, M. A.; Schoenitz, M.; Zhu, X.; Dreizin, E. L. *Combust. Flame* **2005**, *140*, 310.
(4) Sun, J.; Pantoya, M. L.; Simon, S. L. *Thermochim. Acta* **2006**, *444*, 117.
(5) Morgan, A. B.; Wolf, J. D.; Guliants, E. A.; Fernando, K. A. S.; Lewis, W. K. *Thermochim. Acta* **2009**, *488*, 1.
(6) Ermoline, A.; Schoenitz, M.; Dreizin, E.; Yao, N. *Nanotechnology* **2002**, *13*, 638.
(7) Roy, C.; Dubois, C.; Lafleur, P.; Brousseau, P. *Mater. Res. Soc. Symp. Proc.* **2003**, *800*, 79.
(8) Jouet, R. J.; Warren, A. D.; Rosenberg, D. M.; Bellitto, V. J.; Park, K.; Zachariah, M. R. *Chem. Mater.* **2005**, *17*, 2987.
(9) Fernando, K. A. S.; Smith, M. J.; Harruff, B. A.; Lewis, W. K.; Guliants, E. A.; Bunker, C. E. *J. Phys. Chem. C* **2008**, *113*, 500.
(10) Foley, T. J.; Johnson, C. E.; Higa, K. T. *Chem. Mater.* **2005**, *17*, 4086.
(11) Haber, J. A.; Buhro, W. E. *J. Am. Chem. Soc.* **1998**, *120*, 10847.
(12) Chung, S. W.; Guliants, E. A.; Bunker, C. E.; Hammerstroem, D. W.; Deng, Y.; Burgers, M. A.; Jelliss, P. A.; Buckner, S. W. *Langmuir* **2009**, *25*, 8883.
(13) Glotov, O. G.; Zyryanov, V. Y. *Arch. Combust.* **1991**, *11*, 251.
(14) Yang, S.-P.; Tsai, R.-Y. *J. Chem. Educ.* **2006**, *83*, 906.
(15) Kaiser, E. M.; Edmonds, C. G.; Grubb, S. D.; Smith, J. W.; Tramp, D. *J. Org. Chem.* **1971**, *36*, 330.
(16) Chanda, M. In *Introduction to polymer science and chemistry: a problem solving approach*; CRC Press (Taylor & Francis): Boca Raton, FL, 2006; p 601.
(17) Cangiano, D. L.; Odian, G. *Polym. Prepr. (Am. Chem. Soc., Div. Polym. Chem.)* **1991**, *32*, 238.
(18) Burgers, M. A.; Oberle, C. D.; Chung, S. W.; Guliants, E. A.; Kalugotla, V.; Bunker, C. E.; Hammerstroem, D. W.; Jelliss, P. A.; Buckner, S. W. *Am. Chem. Soc., Div. Fuel Chem.* **2010**, *55*, 650.
(19) Dreizin, E. *Prog. Energy Combust. Sci.* **2009**, *35*, 141.
(20) Su, Y.-L.; Wang, J.; Liu, H.-Z. *Langmuir* **2002**, *18*, 5370.
(21) Tedsree, K.; Kong, A. T. S.; Tsang, S. C. *Angew. Chem., Int. Ed. Engl.* **2009**, *48*, 1443.
(22) Fernando, K. A. S.; Smith, M. J.; Harruff, B. A.; Lewis, W. K.; Guliants, E. A.; Bunker, C. E. *J. Phys. Chem. C* **2008**, *113*, 500.